

ACCELERATED COMMUNICATION

G Protein-Coupled Receptors as Direct Targets of Inhaled Anesthetics

YUMIKO ISHIZAWA, RAVINDERNATH PIDIKITI, PAUL A. LIEBMAN, and RODERIC G. ECKENHOFF

Departments of Anesthesia (Y.I., R.P., R.G.E.), Physiology (R.G.E.), and Biochemistry and Biophysics (P.A.L.), University of Pennsylvania Medical Center, Philadelphia, Pennsylvania

Received November 16, 2001; accepted January 31, 2002

This article is available online at <http://molpharm.aspetjournals.org>

ABSTRACT

The molecular pharmacology of inhalational anesthetics remains poorly understood. Despite accumulating evidence suggesting that neuronal membrane proteins are potential targets of inhaled anesthetics, most currently favored membrane protein targets lack any direct evidence for anesthetic binding. We report herein the location of the binding site for the inhaled anesthetic halothane at the amino acid residue level of resolution in the ligand binding cavity in a prototypical G protein-coupled receptor, bovine rhodopsin. Tryptophan fluorescence quenching and direct photoaffinity labeling with [¹⁴C]halothane suggested an interhelical location of halothane with a stoichi-

ometry of 1 (halothane/rhodopsin molar ratio). Radiosequence analysis of [¹⁴C]halothane-labeled rhodopsin revealed that halothane contacts an amino acid residue (Trp265) lining the ligand binding cavity in the transmembrane core of the receptor. The predicted functional consequence, competition between halothane and the ligand retinal, was shown here by spectroscopy and is known to exist *in vivo*. These data suggest that competition with endogenous ligands may be a general mechanism of the action of halothane at this large family of signaling proteins.

The mechanisms of general anesthetic action at the molecular level remain poorly understood, despite their use in millions of patients each year. Understanding the molecular mechanisms by which inhaled anesthetics produce behavioral effects, such as loss of consciousness and analgesia, is thus an important goal with therapeutic implications. Accumulating evidence suggests that these drugs act at multiple neuronal membrane proteins that function as ion channels and neurotransmitter receptors (Franks and Lieb, 1994). However, classification as an anesthetic target requires evidence of direct binding, and most currently favored targets lack any direct evidence for anesthetic binding. One of the major difficulties in demonstrating direct binding is the weak binding energetics of the inhaled anesthetic (Eckenhoff and Johansson, 1997). Weak binding, although consistent with the relatively featureless molecules and the high aqueous EC₅₀ for general anesthesia in mammals (0.2–1.0 mM) (Franks and Lieb, 1994), essentially precludes conventional

radioligand binding studies. Furthermore, there have been few good model systems for studying the actions of inhaled anesthetics in biological membranes (Forman et al., 1997). In addition to plausible roles in central nervous system signaling, it is important for potential model proteins to be available in sufficient abundance and purity to permit direct binding and high-resolution structural studies.

A large superfamily of G protein-coupled receptors (GPCRs) modulates most signaling in central and peripheral nervous systems. In particular, the rhodopsin family of GPCRs includes many neurotransmitter receptors, such as muscarinic acetylcholine, noradrenaline, dopamine, adenosine, and opioid receptors (Baldwin et al., 1997). These receptors have highly conserved regions in the transmembrane portion (Baldwin et al., 1997), and the ligand-receptor interactions in the core formed by the seven α -helices are thought to be similar in the GPCRs of this family (Strader et al., 1994; Ji et al., 1998). Functionally, cholinergic neurotransmission is known to influence awareness, sleep, and learning and memory (Durieux, 1996). The α_2 -adrenergic receptor seems to play a role in antinociceptive responses as well as in the

This work was supported by National Institutes of Health grants GM51595 and EY00012.

ABBREVIATIONS: GPCR, G protein-coupled receptor; RDM, rod disk membranes; MOPS, 3-(*N*-morpholino)propanesulfonic acid; PAGE, polyacrylamide gel electrophoresis; PTH, phenylthiohydantoin; NATA, *N*-acetyl-tryptophan-amide; PKC, protein kinase C.

state of arousal (Bol et al., 1999). In fact, agonists and/or antagonists that work through these GPCRs have been reported to significantly alter anesthetic requirements in humans and animals (Segal et al., 1988; Seitz et al., 1990; Glass et al., 1997; Ishizawa et al., 2000a). Although this might include unrelated, parallel effects on the central nervous system, recent studies show that inhaled anesthetics can interfere with GPCR signaling in vitro (Durieux, 1995; Honemann et al., 1998; Schotten et al., 1998), suggesting direct anesthetic effects.

Halothane, a clinically used volatile anesthetic, has two features that allow monitoring of binding. First, the photolabile carbon-bromine bond allows photolabeling (Eckenhoff and Johansson, 1997); second, the bromine atom can quench intrinsic protein fluorescence if it is near the fluorophore (Johansson et al., 1995). Both features allow determination of location of the anesthetic within the protein matrix. Because the abundance of rhodopsin in native retinal membrane preparation facilitates direct binding approaches, we used bovine rhodopsin as a structural homolog for other neuronal GPCRs to characterize the binding domain for this inhaled anesthetic. We reported previously that halothane binds to rhodopsin but not to its associated G protein (Ishizawa et al., 2000b). In this study, using a higher resolution approach, we provide evidence for halothane binding to the endogenous ligand binding site in rhodopsin.

Materials and Methods

Rod Disk Membranes Preparation. Fresh bovine retinas were dissected in room light. Rod disk membranes (RDM) were prepared by sucrose flotation in isotonic buffer (20 mM MOPS, 100 mM KCl, 6 mM MgCl₂, pH 7.0). Peripheral proteins were stripped by washing in hypotonic buffer (10 mM MOPS, 2 mM MgCl₂, 100 μM GTP, pH 7.0) (Panico et al., 1990). Estimated molar ratio of the protein in the RDM was 24:1 (rhodopsin/transducin) based on the relative mass in SDS-PAGE using reflective density (GS-710; Bio-Rad Laboratories, Hercules, CA). Molar ratio of tryptophan residues was then 12:1 (rhodopsin/transducin). Tryptophan residues in cyclic GMP phosphodiesterase and arrestin were estimated to be lower than 3% and 0.5% of the total residues in RDM, respectively. The RDM were regenerated using 3-fold molar excess of 9-*cis*-retinal (Sigma Chemical Co., St. Louis, MO) for 12 h on ice in the dark followed by a further 1 h incubation at room temperature, as reported previously, to provide almost 100% of chromophore regeneration (Gibson et al., 1998).

Steady-State Fluorescence and Absorption Spectra. All fluorescence measurements were performed with a spectrofluorophotometer (RF-5301PC; Shimadzu Scientific Instruments, Inc. Columbia, MD) using a 10-mm-pathlength quartz cell at 25°C. Bleached and regenerated RDM samples were equilibrated in sodium phosphate buffer (130 mM NaCl and 20 mM Na₂HPO₄, pH 7.0) at a rhodopsin concentration of 0.5 μM with increasing concentrations of halothane (0–15 mM) in a gas-tight 4.0-ml cell. RDM samples were excited at 295 nm to probe tryptophan fluorescence.

For the fluorescence time-based measurements, the RDM samples were equilibrated in sodium phosphate buffer at a rhodopsin concentration of 0.5 μM with increasing concentrations of halothane (0–6.0 mM). Then the RDM were excited with 295 nm light and 3-fold molar excess of 9-*cis*-retinal (1.5 μl) was added to the sample cell (4.0 ml) with continuous stirring. Data were recorded at 330 nm at 30-s intervals for 60 min, with the excitation shutter closed between acquisitions to minimize exposure to the excitation beam. Halothane and 9-*cis*-retinal, the two principle ligands in this study, do not absorb appreciably at the excitation (295 nm) or emission (~330 nm)

wavelength for tryptophan, so inner filter corrections were not performed.

All UV/visible spectra were measured with a spectrophotometer (Cary300Bio; Varian Instruments, Walnut Creek, CA) using a 10-mm-pathlength 1.8-ml quartz cell at 25°C. RDM samples were equilibrated in sodium phosphate buffer at a rhodopsin concentration of 5.0 μM with increasing concentrations of halothane (0–4.0 mM). The time course of the increase in absorbance at 487 nm after addition of 9-*cis*-retinal (3-fold molar excess) was measured for 180 min.

Photoaffinity Labeling of [¹⁴C]Halothane. Bleached and regenerated RDM samples were incubated with [¹⁴C]halothane (2-bromo-2-chloro-1,1,1-[¹⁴C]trifluoroethane; specific activity, 51 mCi/mmol; PerkinElmer Life Sciences, Boston, MA) and with increasing concentrations of unlabeled halothane in isotonic MOPS buffer in 2-ml quartz cuvettes at 25°C. The samples were exposed to 254-nm light at a distance of ~5 mm for 30 s with continuous stirring. The final concentrations in the photolabeling solution were 1.5 μM rhodopsin, 9.7 μM [¹⁴C]halothane, and 0 to 8.5 mM unlabeled halothane. SDS-PAGE of the labeled membranes was performed in modified Laemmli gels, and the gels were stained with Coomassie Brilliant Blue. The relative protein mass in the rhodopsin bands on SDS-PAGE was determined by reflective density. Then rhodopsin bands in the dried gels were excised and dissolved by incubating with 30% hydrogen peroxide at 60°C for 5 h. Stoichiometry of label incorporation into opsin or isorhodopsin was determined in the dissolved gel slices by scintillation counting, and disintegrations per minute were normalized to relative mass of rhodopsin.

For proteolytic digestion and radiosequence analysis, the bleached and regenerated RDM samples were incubated with [¹⁴C]halothane at 0.75 mM in isotonic MOPS buffer. The samples were exposed to 254-nm light for 40 s. The labeled samples were washed with the buffer, and the pellets were then used for proteolytic digestion.

Proteolysis and Radiosequence Analysis. The pellets of the photolabeled RDM were resuspended in 15 mM Tris, 0.1% SDS, pH 8.1. For digestion with *Staphylococcus aureus* glutamyl endopeptidase (V8 protease; ICN Biomedicals Inc., Aurora, OH), V8 protease was added to the final concentration of 1:1 (w/w) protease/rhodopsin into the sample solution and incubated at 37°C for 3 h. For endoprotease Lys-C (EndoLysC) digestion (Roche Applied Science, Indianapolis, IN), EndoLysC was added at ~2 mU:1 μg (protease: rhodopsin), and incubated at 37°C for 6 to 8 hours. The suspension of proteolytic fragments from enzymatic digestion was diluted in sample loading buffer. SDS/PAGE was performed in the modified Laemmli gels, and the gel was subsequently electroblotted to a polyvinylidene difluoride membrane (Problott Membranes; Applied Biosystems, Foster City, CA).

Automated N-terminal sequence analysis was performed on an Applied Biosystems model 473A protein sequencer (Foster City, CA) with an in-line 120A PTH analyzer. Blotted samples were directly loaded onto the chamber, and sequencing was performed using gas-phase trifluoroacetic acid to minimize possible hydrolysis. After conversion of the released amino acids to PTH-amino acids, the suspension was divided into two parts. One portion, approximately 30%, went to the PTH analyzer, whereas the remaining 70% was collected for scintillation counting. Yield of PTH amino acids was calculated from peak height compared with standards using the model 610A Data Analysis Program. Cysteine was not included in the standards. The analysis was done at least twice for each fragment.

Results

Halothane Binding to Opsin and Regenerated Isorhodopsin. Halothane binding to rhodopsin in RDM was initially studied using intrinsic protein fluorescence. Halothane decreased tryptophan fluorescence of the bleached RDM by 80% with a *K_d* value of 2.3 mM (95% CI, 1.8–2.8) (Fig. 1A). Tryptophan fluorescence of the RDM was also

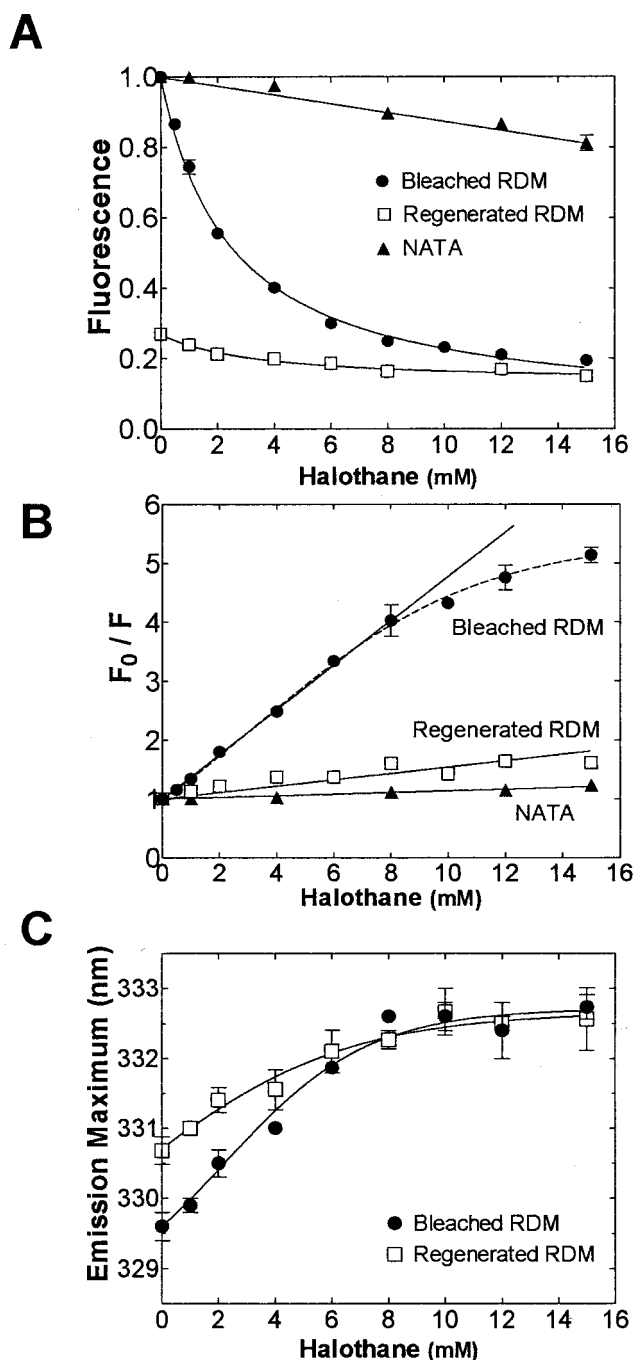


Fig. 1. Halothane effects on tryptophan fluorescence of bleached and regenerated RDM. A, quenching of tryptophan fluorescence by halothane. The data were fitted to the equation; $F = Y_0 - [(Q_{\max} \times [\text{halothane}]) / (K_D + [\text{halothane}])]$, where F is fluorescence intensity, Y_0 is fluorescence intensity in the absence of halothane, Q_{\max} is the maximum fluorescence that can be quenched, and K_D is the dissociation constant for the binding of anesthetic to rhodopsin. Values are means \pm S.E.M ($n = 5$). B, Stern-Volmer plots of halothane quenching. F_0 is the total fluorescence intensity in the absence of halothane. The calculated slope was equated to dynamic parameters according to the modified Stern-Volmer equation: $F_0 / F = 1 + K_{SV} [\text{Halothane}]$. A K_{SV} is $0.38 \pm 0.01 \text{ mM}^{-1}$ for the bleached RDM, $0.05 \pm 0.01 \text{ mM}^{-1}$ for the regenerated RDM, and $0.01 \pm 0.001 \text{ M}^{-1}$ for NATA. Values are means \pm S.E.M ($n = 5$). Curvature at high [halothane] (dashed line) is interpreted as caused by fluorescence arising from halothane inaccessible tryptophan residues. C, changes in the tryptophan emission maximum wavelength. Halothane 15 mM shifts the emission maximum from $329.7 \pm 0.2 \text{ nm}$ to $332.7 \pm 0.1 \text{ nm}$ in the bleached RDM, and from $330.8 \pm 0.2 \text{ nm}$ to $332.6 \pm 0.5 \text{ nm}$ in the regenerated RDM. Values are means \pm S.E.M ($n = 5$).

decreased by nearly 75% upon regeneration of chromophore (isorhodopsin) with 9-*cis*-retinal. In the regenerated RDM, halothane further decreased tryptophan fluorescence with a K_d value of 4.1 mM (95% CI, 1.0–6.4), but only by 11% (Fig. 1A). *N*-Acetyl-tryptophan-amide (NATA) was used as a control for random collisional quenching of soluble tryptophan. Halothane decreased tryptophan fluorescence for NATA in a linear fashion, with a maximum quenching of $19 \pm 2\%$ at 15 mM. Stern-Volmer plots for these halothane effects are shown in Fig. 1B. The tryptophan emission wavelength maximum of bleached RDM was $329.6 \pm 0.2 \text{ nm}$, and regeneration with 9-*cis*-retinal shifted it to $330.8 \pm 0.2 \text{ nm}$. Halothane red-shifted the emission maximum in both bleached and regenerated RDM (Fig. 1C). Because fluorescence quenching by halothane is considered a short-range phenomenon (Basu et al., 1993), these changes indicate that halothane binds near most of the five tryptophan residues present in this molecule and that those residues are located in hydrophobic environments.

The reversibility of the effects of halothane on tryptophan fluorescence was examined to evaluate whether halothane-induced aggregation or precipitation of rhodopsin might be responsible for the observed tryptophan quenching. RDM samples in the presence of halothane was first measured fluorometrically, and then exposed to a stream of argon for 90 min in the dark to remove the anesthetic (Roberts and Dunker, 1993). These samples regained $105 \pm 4\%$ and $90 \pm 10\%$ of its tryptophan fluorescence for 2 mM and 12 mM halothane, respectively, compared with a control sample treated in the same manner (mean \pm S.E.M., $n = 3$ for each). The tryptophan emission maximum after the treatment was not different from the value of the control.

To evaluate the environments surrounding the tryptophan residues in rhodopsin, experiments were performed with a water-soluble quencher, acrylamide. Acrylamide weakly quenched tryptophan fluorescence for bleached RDM and regenerated RDM (17% and 36%, respectively, at 0.8 M) in the absence of halothane (Fig. 2A). Acrylamide also caused the emission maximum to shift from $329.6 \pm 0.2 \text{ nm}$ to $326.8 \pm 0.1 \text{ nm}$ in the bleached RDM, and from $330.8 \pm 0.2 \text{ nm}$ to $326.1 \pm 0.2 \text{ nm}$ in the regenerated RDM. Halothane had no significant effect on this acrylamide-sensitive component (Fig. 2B), indicating that halothane does not bind near the more exposed tryptophan residue accessible to acrylamide. The recently reported crystal structure of bovine rhodopsin identifies Trp35 as the most solvent exposed tryptophan residue (Palczewski et al., 2000), and thus Trp35 is a reasonable candidate for quenching by acrylamide.

Similar quenching behavior suggests that halothane and retinal binding sites may overlap. To test for the predicted competition between halothane and the ligand retinal, we photolabeled RDM with [^{14}C]halothane in the presence and absence of bound retinal. Incorporation of [^{14}C]halothane into opsin (the receptor protein without bound retinal) was significantly inhibited by unlabeled halothane with an IC_{50} value of 1.1 mM (95% CI, 0.8–1.6) and a Hill coefficient of -1.4 (95% CI, $-2.1 \sim -0.8$) (Fig. 3). In regenerated isorhodopsin, although the IC_{50} was essentially unaltered (1.1 mM), label incorporation was significantly decreased. The calculated maximum stoichiometry was 1.08 (halothane/rhodopsin molar ratio) in opsin and 0.28 in isorhodopsin.

Halothane Binds to the Ligand Binding Site. The fluorescence and photoaffinity labeling data both suggest that halothane binds close to the ligand binding site in the transmembrane core of rhodopsin. However, hydrophobic volatile anesthetics have been shown to preferentially bind to the lipid-protein interface as well (Tang et al., 2000), which might alter fluorescence and ligand binding allosterically. Accordingly, we tested this possibility by performing proteolysis and radiosequence analysis of [^{14}C]halothane-photolabeled rhodopsin. A small fragment from enzymatic digestion with V8 protease, previously shown to include the site where photoreactive retinal analogs are incorporated (Zhang et al., 1994), was used (Fig. 4A, V8-S). Release of ^{14}C was observed in cycle 26, indicating halothane photoincorporation at Trp265 (Fig. 4B). In the same fragment from regenerated isorhodopsin (retinal-bound), ^{14}C release at Trp265 was significantly smaller than that released from opsin. Because the efficiency of Edman degradation is not 100%, the repetitive

yield results in a well-known lag of the residue release (and therefore cpm), which grows in magnitude with the number of cycles. Therefore, most of the cpm release measured at cycle 27 and the cycles thereafter represents lag from cycle 26 and is unlikely to represent labeling of Leu266.

Because we predicted that the acrylamide-sensitive, halothane-resistant component of the tryptophan fluorescence arose from Trp35, we subjected a proteolytic fragment containing this residue to radiosequencing as well (Fig. 4A, EndoLysC). In this EndoLysC fragment, there was no significant release of radioactivity in close vicinity to Trp35 in opsin or in isorhodopsin (Fig. 4C), confirming the importance of the more buried site, and eliminating the trivial explanation of photochemical selectivity being responsible for Trp265 labeling. Additionally, the present radiosequencing through helices 1 and 6 did not provide evidence that halothane preferentially binds to the residues at the lipid-protein interface.

The crystal structure of bovine rhodopsin confirms that Trp265 lines the core of the α -helical bundle (Palczewski et al., 2000). Trp265 is known to interact with retinal (Lin and Sakmar, 1996; Kochendoerfer et al., 1997; Palczewski et al., 2000) and to play an important role in rhodopsin regeneration (Reeves et al., 1999). To illustrate the relationship between the retinal cavity formed in the interhelical space of rhodopsin and the photolabeled residues, the Gravitational Radiation Analysis and Simulation Package (GRASP; <http://www.lsc-group.phys.uwm.edu/~ballen/grasp-distribution/>) was used to render the cavity surface on the crystal structure of rhodopsin with retinal removed (Fig. 5) (Nicholls et al., 1991). This cavity is measured to be 428 \AA^3 , sufficient volume to accommodate at least two halothane molecules (volume of $\sim 130 \text{ \AA}^3$) but it is likely to at least partially collapse on removal of retinal. No other suitable cavity exists in the protein structure.

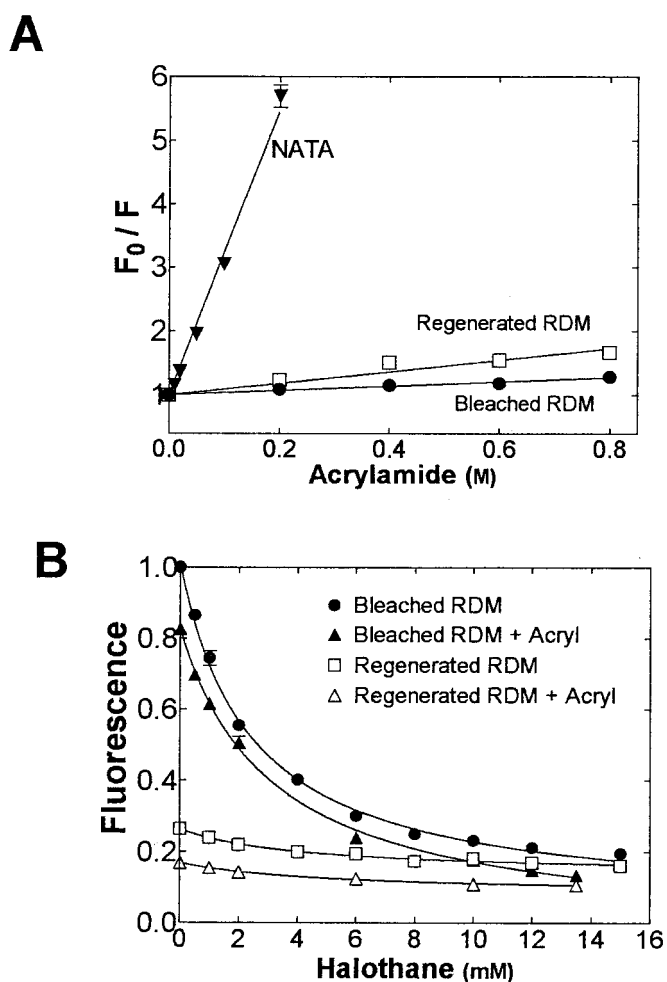


Fig. 2. Effects of a water-soluble quencher acrylamide on tryptophan fluorescence of the bleached and regenerated RDM, and NATA. A, Stern-Volmer plots of acrylamide quenching. The data were fitted to the modified Stern-Volmer equation: $F_0/F = 1 + K_{SV} [\text{Acrylamide}]$. A K_{SV} is $0.34 \pm 0.02 \text{ M}^{-1}$ for the bleached RDM, $0.94 \pm 0.08 \text{ M}^{-1}$ for the regenerated RDM, and $22.9 \pm 0.6 \text{ M}^{-1}$ for NATA. Values are means \pm S.E.M ($n = 4$). B, the effects of acrylamide 0.8 M on the halothane quenching of tryptophan fluorescence for the bleached and regenerated RDM, containing $0.5 \mu\text{M}$ opsin and isorhodopsin, respectively. The data were fitted to the equation; $F = Y_0 - [(Q_{\text{max}} \times [\text{halothane}]) / (K_D + [\text{halothane}])]$. Values are means \pm S.E.M ($n = 4$).

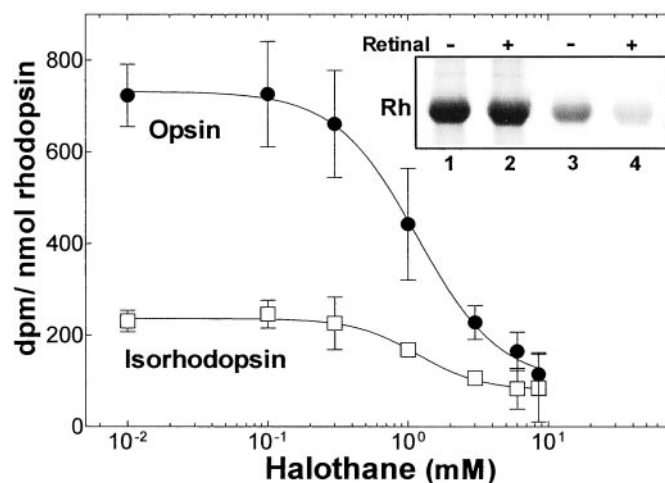


Fig. 3. Photoaffinity labeling of [^{14}C]halothane to bleached and regenerated RDM. Protection from [^{14}C]halothane labeling by unlabeled halothane is shown in opsin and isorhodopsin recovered from the gel of the bleached RDM and the regenerated RDM, respectively. Photoincorporation is presented as disintegrations per minute per nanomolar rhodopsin. The data were fitted to sigmoid dose-response curves (variable slopes) with nonlinear least-squares regression. Values are means \pm S.E.M. ($n = 3$). Inset shows rhodopsin band (Rh) in the stained gel electrophoresis of the bleached RDM (lane 1) and the regenerated RDM (lane 2). Lanes 3 and 4 are the resulting autoradiogram, which show dominant photoincorporation into the opsin band in the bleached RDM (lane 3) but significantly less incorporation into the isorhodopsin band in the regenerated RDM (lane 4).

Competition between Halothane and the Ligand. Finally, to confirm the predicted competitive interaction between halothane and the ligand retinal, retinal binding kinetics was monitored by the specific absorption wavelength for isorhodopsin after the addition of 9-*cis*-retinal. Halothane significantly prolonged isorhodopsin formation in a concentration-dependent manner, indicating that halothane inhibits retinal binding to opsin (Fig. 6; Table 1). The kinetics of

the fluorescence decrease produced by retinal binding was also prolonged in the presence of halothane (Table 1). These data not only confirm competition between halothane and retinal at the retinal binding site in rhodopsin but also predict specific *in vivo* functional changes (see *Discussion*). Although we noted that the increase in the absorbance was slower than the fluorescence decrease, the spectroscopic probes report different endpoints of the regeneration process of isorhodopsin, and the data suggest that quenching of tryptophan fluorescence is established at an earlier stage of chromophore regeneration.

Discussion

Using several different approaches, we have shown here that a general inhaled anesthetic binds to the endogenous ligand binding site and competitively inhibits the ligand binding in a prototypical GPCR. Photoincorporation of

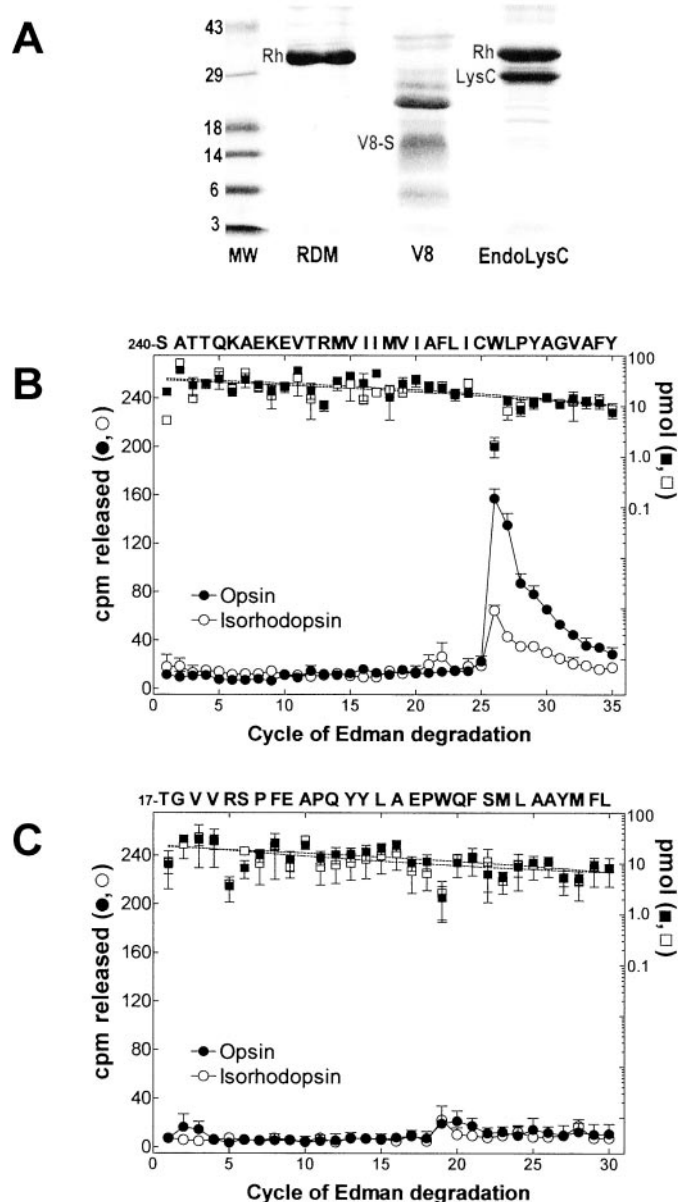


Fig. 4. Radiosequence analysis of the proteolytic fragments of rhodopsin. A, gel electrophoresis of the RDM, the proteolytic fragments from V8 protease digestion (V8), and those from endoproteinase Lys-C (EndoLysC). Indicated on the left are rhodopsin (Rh), a fragment from V8 digestion (V8-S), and a EndoLysC digest (LysC). Lane MW consists of size markers in kilodaltons. B, Sequence analysis of V8-S from photolabeled opsin and isorhodopsin. Significant release of the cpm in opsin is observed at cycle 26, representing Trp265. In isorhodopsin, there is a radioactive peak at Trp265, but the cpm released is significantly lower than those in opsin. C, Sequence analysis of LysC fragment from opsin and isorhodopsin. There is no significant release of the cpm in the sequenced residues from opsin or isorhodopsin. For both B and C, primary sequence for each fragment is shown on top axes.

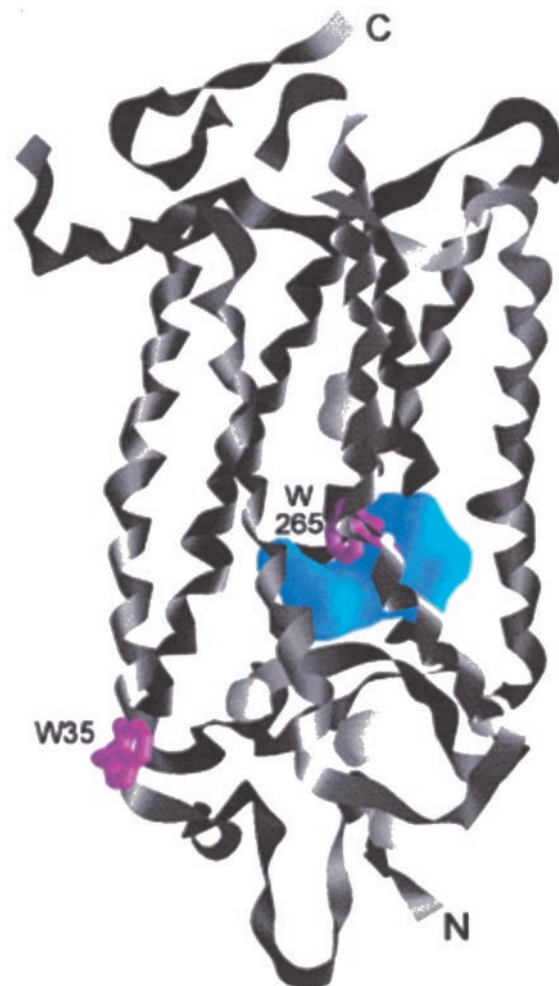


Fig. 5. The structure of bovine rhodopsin (Palczewski et al., 2000) is viewed from within the membrane looking from helices 6 and 7. The intracellular side of the molecule is at the top. 11-*cis*-Retinal is removed from the structure. Trp35 (helix 1) and Trp265 (helix 6) are shown in magenta. The blue object is a surface rendering of the cavity in the transmembrane core. The volume of this cavity is 428 Å³, and the surface area is 376 Å². Trp265 is closely located to this cavity. The cavity analysis was done using a probe of 1.4-Å diameter using GRASP (Nicholls et al., 1991). The surfaces of the small cavities detected are shown with light gray. The figure was produced with Protein Data Bank structure file (1F88).

[¹⁴C]halothane at Trp265 indicates unambiguous location of halothane in the interhelical core in opsin, which is consistent with the photoaffinity stoichiometry of 1 for halothane in opsin. The crystal structure of bovine rhodopsin has confirmed that the ligand-binding cavity can accommodate halothane in the core formed by the α -helical bundle.

Competition between halothane and the ligand retinal predicts that the anesthetic may interfere with retinal binding in a functionally apparent manner. Indeed, the functional importance of this binding interaction is shown by a recent *in vivo* finding that rhodopsin regeneration in mice and rats was significantly inhibited under halothane anesthesia at 1.5–1.8% (v/v), corresponding to about 0.4 mM at 37°C (Keller et al., 2001). Dark adaptation of vision, in which retinal chromophore regeneration plays an important role, was also reported to be retarded in humans and monkeys under halothane anesthesia (van Norren and Padmos, 1975). Our data are consistent with other studies showing functional effects of volatile anesthetics on GPCRs *in vitro* as well. For example, halothane competitively inhibited muscarinic and thromboxane A₂ signaling monitored with Ca²⁺-

activated Cl⁻ currents in *Xenopus laevis* oocytes, but it had no effect on intracellular signaling pathways, indicating that halothane interacts with the receptor and/or receptor-G protein coupling (Durieux, 1995; Honemann et al., 1998). Halothane also decreased ligand binding affinity for the β -adrenergic receptor in rat myocardium, and reduced positive inotropic potency of its agonist (Schotten et al., 1998). Although the effect of inhaled anesthetics on protein kinase C (PKC) or on PKC phosphorylation sites of the receptor was suggested in the metabotropic glutamate receptor, direct interactions of anesthetics with the hydrophobic domain of the receptor cannot be eliminated because of the lack of the concentration-effect relationships between PKC inhibitors/activators and anesthetics (Minami et al., 1998). Further studies may need to define anesthetic actions at the downstream of a variety of GPCR signaling cascades.

It is interesting that the effective concentrations of halothane in these previous *in vivo* and *in vitro* studies seem to be lower than those describing the binding relationship in this study (1.1–2.3 mM, equivalent to the gaseous concentration of 4 to 9%). Dark adaptation was significantly altered at the lowest halothane concentration of 0.2% (van Norren and Padmos, 1975). Halothane inhibited muscarinic signaling in oocytes with an IC₅₀ of 0.3 mM (Durieux, 1995). These differences probably reflect the enormous signal amplification and the well-known displacement of concentration-effect curves from receptor-occupancy profiles in the GPCR systems (Ross, 1996). In this context, it is particularly interesting that halothane almost completely inhibited retinal regeneration in mice at 1.8% (Keller et al., 2001), the same phenomenon that we observed using membrane preparations at higher halothane concentrations. The explanation for this difference in halothane sensitivity is not clear, but could be caused by species differences or by altered functioning of this receptor in the *in vitro* membrane preparation.

The site of halothane binding identified in this study may represent a common anesthetic binding motif in many GPCRs. First, the residue identified as most contributing to the site for halothane, Trp265, is one of the most conserved residues in more than 199 unique sequences of the GPCRs in the rhodopsin family (Baldwin et al., 1997). Second, a similar interhelical domain is created with a sufficient number of conserved residues in the transmembrane portion in other GPCRs (Baldwin et al., 1997). It is interesting that most of these highly conserved residues face the interior of the molecule in the crystal structure of rhodopsin (Palczewski et al., 2000), confirming a similar molecular environment in the

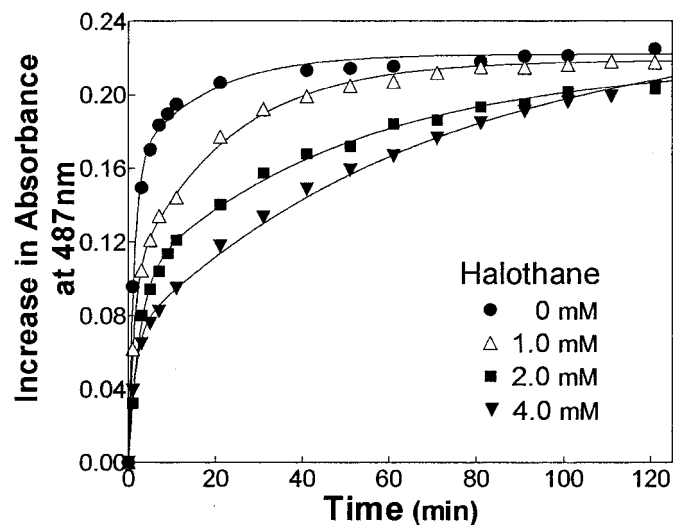


Fig. 6. Effects of halothane on retinal binding kinetics. Retinal binding to opsin in the RDM was monitored by the increase in the specific absorption wavelength for isorhodopsin after addition of 9-*cis*-retinal in the dark. Halothane did not affect the baseline spectrum (700–350 nm) for the bleached RDM, and this baseline spectrum was subtracted from subsequent spectra after addition of retinal. The 3-fold molar excess of 9-*cis*-retinal itself has an absorption peak at 380 nm and its absorbance was 0.013 at 487 nm. The curves through the data points were generated using a two-phase exponential association.

TABLE 1

Effects of halothane on retinal binding kinetics

Half-times of retinal binding kinetics monitored by the increase in the absorbance and the fluorescence decrease. For the increase in the absorbance, the data are fitted to a two-phase exponential association. For the fluorescence decrease, the data were fitted to a two-phase exponential decay. Values are means \pm S.E.M. ($n = 5$ for absorbance, $n = 4$ for fluorescence). All fits showed an R^2 value > 0.99 .

Halothane	0.0 mM	1.0 mM	2.0 mM	4.0 mM	6.0 mM
Absorbance Increase Half-Time					
T1 (s)	47 \pm 6	53 \pm 2	63 \pm 5	76 \pm 7*†	
T2 (min)	17 \pm 2	23 \pm 4	25 \pm 2	35 \pm 6*	
Fast component (%)	68 \pm 3	57 \pm 7*	50 \pm 3*	38 \pm 2*†	
Fluorescence Decrease Half-Time					
T1 (s)	8.0 \pm 0.6		9.3 \pm 0.5	12.4 \pm 1.2*‡	13.6 \pm 1.0*‡
T2 (min)	3.4 \pm 0.3		5.3 \pm 0.5	6.8 \pm 0.9*	12.2 \pm 1.1*‡

* $P < 0.05$ compared with the absence of halothane [one-way analysis of variance (ANOVA) followed by Student-Neuman-Keuls test].

† $P < 0.05$ compared with halothane 1.0 mM (one-way ANOVA followed by Student-Neuman-Keuls test).

‡ $P < 0.05$ compared with halothane 2.0 mM (one-way ANOVA followed by Student-Neuman-Keuls test).

core in these GPCRs. Furthermore, with the use of designed four- α -helical bundles (Johansson et al., 1998, 2000), and other soluble proteins with hydrophobic cavities (Eckenhoff et al., 2000; Eriksson et al., 1992), it has been shown that preformed accessible cavities are important features to facilitate anesthetic binding. Although inhaled anesthetics have divergent chemical structures, the molecules are relatively small (90–160 Å³) and have few interactive atoms or groups to provide much selectivity, compared with other molecules that interact with GPCRs, such as biogenic amines and retinal. All these data support the notion that inhaled anesthetic binding in the interhelical core is a feature of general significance in the GPCR family.

A common binding motif in this class of receptor may also suggest a common mechanism of action of inhaled anesthetics. Although several distinct modes of ligand-receptor interactions are reported for GPCRs, small ligands, such as biogenic amines, eicosanoids, enter and bind in the transmembrane core of their GPCRs as retinal does (Strader et al., 1994; Ji et al., 1998). Covalent attachment of the ligand is indeed unique to rhodopsin, but the binding site for catecholamine in the β -adrenergic receptor is thought to be remarkably similar to the binding site for retinal in rhodopsin (Strader et al., 1994; Sakmar, 1998). Cholinergic ligands have also been reported to interact with aromatic as well as polar residues, such as tyrosine, in the core of the muscarinic receptor (Hulme et al., 1999). Our results thus suggest that disruption of signal transduction through competition with endogenous ligands in the core may be a common mechanism of the action of an inhaled anesthetic like halothane at these GPCRs. Moreover, it has been reported that the ligands that bind to the transmembrane core of the metabotropic glutamate receptor, another family of the GPCRs, allosterically inhibit receptor signaling after agonist binding to the extracellular domain (Litschig et al., 1999; Pagano et al., 2000). This suggests that anesthetic occupancy of this core region may have both competitive and allosteric effects on receptor function. Key features of general anesthesia, such as loss of consciousness and antinociception, as well as anesthetic “side” effects, which include a multitude of cardiovascular and autonomic features, could be explained by a wide spectrum of the roles of GPCR signaling in the central and peripheral nervous systems.

It is important to note that there are striking differences in the effective concentrations between inhaled anesthetics and other pharmacological agents. For example, in contrast to the aqueous EC₅₀ of inhaled anesthetics, ranging between 0.2 and 1.0 mM, opioids and benzodiazepines are effective in nanomolar concentrations. This has led to the interpretation that the inhaled anesthetics may interact with multiple protein sites to produce anesthetic state. Our present data also suggest possible interactions of inhaled anesthetics with other neuronal membrane proteins as well as GPCRs. Because α -helical bundles are a commonly found motif in many membrane proteins, occupancy of interhelical cavities could cause changes in helical arrangement, disruption of oligomerization equilibrium, or alteration in dynamic behavior, all of which may further explain divergent physiological effects of these widely used drugs.

Acknowledgments

We thank Dr. Jonas S. Johansson and Prof. David E. Longnecker for helpful discussions and continuous encouragement, Dr. David C. Chiara and Prof. Jonathan B. Cohen for the help of sequence analysis, and Kin Chan, Christina Reilly, and Robert Sharp for expert technical assistance.

References

- Baldwin JM, Schertler GF, and Unger VM (1997) An alpha-carbon template for the transmembrane helices in the rhodopsin family of G-protein-coupled receptors. *J Mol Biol* **272**:144–164.
- Basu G, Anglos D, and Kuki A (1993) Fluorescence quenching in a strongly helical peptide series: the role of noncovalent pathways in modulating electronic interactions. *Biochemistry* **32**:3067–3076.
- Bol CJ, Vogelaar JP, and Mandema JW (1999) Anesthetic profile of dexmedetomidine identified by stimulus-response and continuous measurements in rats. *J Pharmacol Exp Ther* **291**:153–160.
- Durieux ME (1995) Halothane inhibits signaling through m1 muscarinic receptors expressed in *Xenopus* oocytes. *Anesthesiology* **82**:174–182.
- Durieux ME (1996) Muscarinic signaling in the central nervous system. Recent developments and anesthetic implications. *Anesthesiology* **84**:173–189.
- Eckenhoff RG and Johansson JS (1997) Molecular interactions between inhaled anesthetics and proteins. *Pharmacol Rev* **49**:343–367.
- Eckenhoff RG, Peterson CE, Ha C-E, and Bhagavan NV (2000) Inhaled anesthetic binding sites in human serum albumin. *J Biol Chem* **275**:30439–30444.
- Eriksson AE, Baase WA, Wozniak JA, and Matthews BW (1992) A cavity-containing mutant of T4 lysozyme is stabilized by buried benzene. *Nature (Lond)* **355**:371–373.
- Forman SA, Raines DE, and Miller KW (1997) The interactions of general anesthetics with membranes, in *Anesthesia: Biologic Foundations* (Yaksh TL, Lynch CI, Zepol WM, Maze M, Biebuyck JF, and Saidman LJ eds), pp 5–18, Lippincott-Raven Publishers, Philadelphia.
- Franks NP and Lieb WR (1994) Molecular and cellular mechanisms of general anaesthesia. *Nature (Lond)* **367**:607–614.
- Gibson SK, Parkes JH, and Liebman PA (1998) Phosphorylation stabilizes the active conformation of rhodopsin. *Biochemistry* **37**:11393–8.
- Glass PS, Gan TJ, Howell S, and Ginsberg B (1997) Drug interactions: volatile anesthetics and opioids. *J Clin Anesth* **9**:18S–22S.
- Honemann CW, Nietgen GW, Podranski T, Chan CK, and Durieux ME (1998) Influence of volatile anesthetics on thromboxane A2 signaling. *Anesthesiology* **88**:440–451.
- Hulme EC, Lu ZL, Ward SD, Allman K, and Curtis CA (1999) The conformational switch in 7-transmembrane receptors: the muscarinic receptor paradigm. *Eur J Pharmacol* **375**:247–260.
- Ishizawa Y, Ma H-C, Dohi S, and Shimonaka H (2000a) Effects of cholinomimetic injection into the brain stem reticular formation on halothane anesthesia and antinociception in rats. *J Pharmacol Exp Ther* **293**:845–851.
- Ishizawa Y, Sharp R, Liebman PA, and Eckenhoff RG (2000b) Halothane binding to a G protein coupled receptor in retinal membranes by photoaffinity labeling. *Biochemistry* **39**:8497–8502.
- Ji TH, Grossmann M, and Ji I (1998) G protein-coupled receptors. I. Diversity of receptor-ligand interactions. *J Biol Chem* **273**:17299–302.
- Johansson JS, Eckenhoff RG, and Dutton PL (1995) Binding of halothane to serum albumin demonstrated using tryptophan fluorescence. *Anesthesiology* **83**:316–324.
- Johansson JS, Gibney BR, Rabanal F, Reddy KS, and Dutton PL (1998) A designed cavity in the hydrophobic core of a four-alpha-helix bundle improves volatile anesthetic binding affinity. *Biochemistry* **37**, 1421–1429.
- Johansson JS, Scharf D, Davies LA, Reddy KS, and Eckenhoff RG (2000) A designed four-alpha-helix bundle that binds the volatile general anesthetic halothane with high affinity. *Biophys J* **78**:982–993.
- Keller C, Grimm C, Wenzel A, Hafezi F, and Reme CE (2001) Protective effect of halothane anesthesia on retinal light damage: Inhibition of metabolic rhodopsin regeneration. *Invest Ophthalmol Vis Sci* **42**:476–480.
- Kochendoerfer GG, Wang Z, Oprian DD, and Mathies RA (1997) Resonance Raman examination of the wavelength regulation mechanism in human visual pigments. *Biochemistry* **36**:6577–6587.
- Lin SW and Sakmar TP (1996) Specific tryptophan UV-absorbance changes are probes of the transition of rhodopsin to its active state. *Biochemistry* **35**:11149–11159.
- Litschig S, Gasparini F, Rueegg D, Stoehr N, Flor PJ, Vranesic I, Prezeau L, Pin J-P, Thomsen C, and Kuhn R (1999) CPCCOEt, a noncompetitive metabotropic glutamate receptor 1 antagonist, inhibits receptor signaling without affecting glutamate binding. *Mol Pharmacol* **55**:453–461.
- Minami K, Gereau RW 4th, Minami M, Heinemann SF and Harris RA (1998) Effects of ethanol and anesthetics on type 1 and 5 metabotropic glutamate receptors expressed in *Xenopus laevis* oocytes. *Mol Pharmacol* **53**:148–156.
- Nicholls A, Sharp KA, and Honig B (1991) Protein folding and association: insights from the interfacial and thermodynamic properties of hydrocarbons. *Proteins* **11**:281–296.
- von Norren D and Padmos P (1975) Cone dark adaptation: the influence of halothane anesthesia. *Invest Ophthalmol Vis Sci* **14**:212–227.
- Pagano A, Ruegg D, Litschig S, Stoehr N, Stierlin C, Heinrich M, Floersheim P, Prezeau L, Carroll F, Pin J-P, et al. (2000) The non-competitive antagonists 2-methyl-6-(phenylethyl)pyridine and 7-hydroxyiminocycopropan [b]chromen-1a-carboxylic acid ethyl ester interact with overlapping binding pockets in the transmembrane region of group I metabotropic glutamate receptors. *J Biol Chem* **275**:33750–33758.

- Palczewski K, Kumasaka T, Hori T, Behnke CA, Motoshima H, Fox BA, LeTrong IL, Teller DC, Okada T, Stenkamp RE, et al. (2000) Crystal structure of rhodopsin: A G protein-coupled receptor. *Science (Wash DC)* **289**:739–745.
- Panico J, Parkes JH, and Liebman PA (1990) The effect of GDP on rod outer segment G-protein interactions. *J Biol Chem* **265**:18922–18927.
- Reeves PJ, Hwa J, and Khorana HG (1999) Structure and function in rhodopsin: kinetic studies of retinal binding to purified opsin mutants in defined phospholipid-detergent mixtures serve as probes of the retinal binding pocket. *Proc Natl Acad Sci USA* **96**:1927–1931.
- Roberts LM and Dunker AK (1993) Structural changes accompanying chloroform-induced contraction of the filamentous phage fd. *Biochemistry* **32**:10479–10488.
- Ross EM (1996) Pharmacodynamics: Mechanisms of drug action and the relationship between drug concentration and effect, in *Goodman & Gilman's The Pharmacological Basis of Therapeutics*. (Hardman JG, Limbird LE, Molinoff PB, Ruddon RW, and Gilman AG eds) pp 29–41, McGraw-Hill, New York.
- Sakmar TP (1998) Rhodopsin: a prototypical G protein-coupled receptor. *Prog Nucl Acid Res Mol Biol* **59**:1–34.
- Schotten U, Schumacher C, Sigmund M, Karlein C, Rose H, Kammermeier H, Sivarajan M, and Hanrath P (1998) Halothane, but not isoflurane, impairs the beta-adrenergic responsiveness in rat myocardium. *Anesthesiology* **88**:1330–1339.
- Segal IS, Vickery RG, Walton JK, Doze VA, and Maze M (1988) Dexmedetomidine diminishes halothane anesthetic requirements in rats through a postsynaptic alpha 2 adrenergic receptor. *Anesthesiology* **69**:818–823.
- Seitz PA, ter Riet M, Rush W and Merrell WJ (1990) Adenosine decreases the minimum alveolar concentration of halothane in dogs. *Anesthesiology* **73**:990–994.
- Strader CD, Fong TM, Tota MR, Underwood D, and Dixon RA (1994) Structure and function of G protein-coupled receptors. *Annu Rev Biochem* **63**:101–132.
- Tang P, Eckenhoff RG, and Xu Y (2000) General anesthetic binding to gramacidin: the structural requirements. *Biophys J* **78**:1804–1809.
- Zhang H, Lerro KA, Yamamoto T, Lien TH, Sastry L, Gawinowicz MA, and Nakanishi K (1994) The location of the chromophore in rhodopsin: A photoaffinity study. *J Am Chem Soc* **116**:10165–10173.

Address correspondence to: Dr. Yumiko Ishizawa, Department of Anesthesia, University of Pennsylvania Medical Center, 3400 Spruce Street, 7 Dulles, Philadelphia, PA 19104-4283. E-mail: ishizawa@mail.med.upenn.edu
